Oncolytic virotherapy - analysis, design, models

Bhatt, Darshak

DOI:
10.33612/diss.859671389

CHAPTER 5

Oncolytic alphavirus-induced extracellular vesicles counteract the immunosuppressive effect of melanoma-derived extracellular vesicles

Darshak K. Bhatt[1,2], Annemarie Boerma[1], Silvina Odete Bustos[2,3], Andréia Hanada Otake[2,3], Alexis Germán Murillo Carrasco[2,3], Patrícia Pintor dos Reis[4], Roger Chammas[2,3*], Toos Daemen[1*], Luciana N.S. Andrade[2,3*]

1 Department of Medical Microbiology and Infection Prevention, University Medical Center Groningen, University of Groningen, 9713 AV Groningen, the Netherlands

2 Center for Translational Research in Oncology, Instituto do Câncer do Hospital das Clínicas da Faculdade de Medicina da Universidade de São Paulo, São Paulo, CEP 01246-000, Brazil

3 Comprehensive Center for Precision Oncology, Universidade de São Paulo, São Paulo, Brazil.

4 Department of Surgery and Orthopedics and Experimental Research Unity (UNIPEX), Faculdade de Medicina, Universidade Estadual Paulista (UNESP), Botucatu 18618-687, Brazil.

*Corresponding author

Submitted

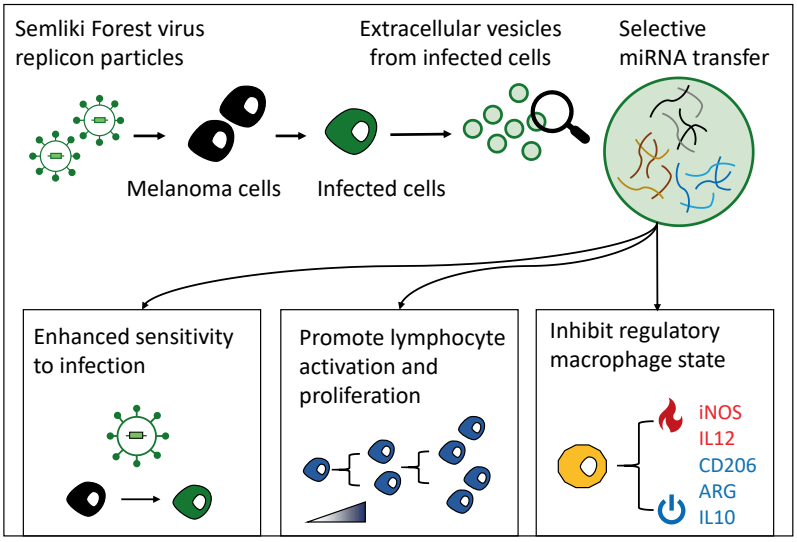

Abstract

Extracellular vesicles (EVs) mediated communication by cancer cells contributes towards the pro-tumoral reprogramming of the tumor microenvironment. Viral infection has been observed to alter the biogenesis and cargo of EVs secreted from host cells in the context of infectious biology. However, the impact of oncolytic viruses on the cargo and function of EVs released by cancer cells remains unknown. Here we show that upon oncolytic virotherapy with Semliki Forest virus-based replicon particles (rSFV), metastatic melanoma cells release EVs with a distinct biochemical profile and do not lead to suppression of immune cells. Specifically, we demonstrate that viral infection causes a differential loading of microRNAs in EVs in addition to changes in their physical features. EVs derived from cancer cells potentially suppress splenocyte proliferation and induce regulatory macrophages. In contrast, EVs obtained from rSFV-infected cells did not exhibit such effects. Our results thus show that rSFV infection induces changes in the immunomodulatory properties of melanoma EVs which may contribute to enhancing the therapeutic efficacy of virotherapy. Finally, our study suggests that using an oncolytic virus capable of a single-round of infection allows the analysis of EVs secreted from infected cells while preventing interference from extracellular virus particles.

Keywords: extracellular vesicles, oncolytic virus, immunomodulatory, melanoma

Introduction

Tumor-derived extracellular vesicles (EVs) have been identified as key players in the regulation of tumor-immune interactions and cancer progression. EVs are produced by all cell types and are known to originate from endosomes and/or the cellular plasma membrane.[1] These vesicles serve as vehicles for transporting bioactive materials, such as proteins, lipids, and genetic material, to recipient cells, influencing various aspects of their function and response.[1,2] This has important implications for oncolytic viruses used in cancer treatment as viral infection may impact cellular communication by regulating the biogenesis and cargo of tumor-derived EVs.[3–5] Virotherapy-induced changes in EV composition, may for example result in regulating the phenotype of recipient immune cells, ultimately affecting therapeutic outcomes. Therefore, understanding the extent to which oncolytic viruses influence the characteristics of EVs remains a crucial area of research.

Previous research has investigated various aspects related to the interaction between EVs and viruses. These studies have explored strategies of viruses encapsulating within EVs to improve delivery and evade antiviral antibodies,[6,7] how EVs allow capsid-independent transfer of viral genomes between cells,[8,9] the differential sorting of microRNA in EVs from infected cells,[10] and the possibility of exploiting EV-mediated communication to induce systemic immunity[11] or sensitize cancer cells to virotherapy.[10,12] However, it has been noted that evaluation of EVs secreted from virus-infected cells is challenging due to the similarities in size and biochemical features between viruses and vesicles,[13,14] such as the presence of a lipid layer envelope containing cellular membrane proteins, as well as their use of similar secretory pathways for extracellular release and fusion with recipient cells.[13] Furthermore, the presence of oncolytic virus within EVs has been found to induce immune-independent abscopal effects by directly mediating cytotoxic activity to distal tumors.[15] This emphasizes the need for careful isolation and characterization of EVs isolated from virus-infected cells while avoiding the presence of extracellular virus particles.

In order to prevent the infected cells from producing new virus particles, we employed the use of recombinant oncolytic Semliki Forest virus capable of a single round of infection. Semliki Forest virus (SFV) is a positive-stranded RNA virus.

The RNA genome of SFV is a replicon, meaning self-replicating, as it encodes non-structural proteins responsible for RNA replication and translation. Recombinant SFV (rSFV) replicon particles can be produced through the use of a two-helper RNA system where the genes encoding viral structural proteins are expressed from an independent RNA molecule devoid of a viral-packaging signal, thus ensuring that the infected cells do not continue to produce virus.[16–18] This allows for the isolation and characterization of tumor EVs without extracellular virus-contamination.

Tumor EVs play an active role in the dynamic tumor-immune signaling occurring in the tumor microenvironment. Similar to various other cancer types, EVs from melanoma have been found to promote cancer survival through pro-tumoral and immunoregulatory mechanisms.[2,19,20] Multiple studies have now shown that melanoma EVs, especially exosomes (or small vesicles, 30-150 nm sized EVs) of the B16F10 model, can promote tumor progression and immune evasion through transfer of survival-promoting signals,[21] presence of immunoregulatory signals,[22,23] and neutralization of checkpoint inhibitors.[24] Therefore, we used the B16F10 model to study changes in the functional profile of melanoma EVs by rSFV-replicon particles. The ability of EVs secreted from rSFV-infected cancer cells to regulate the phenotype of recipient cancer cells and immune cells was systematically investigated. Specifically, we first assessed the difference in physical features of EVs from rSFV-infected cells. Next, we studied the survival of cancer cells, activation of lymphocytes, and phenotypic polarization of macrophages in response to EVs from rSFV-infected or non-infected cells. Finally, we identified the differentially enriched microRNA cargo in EVs from rSFV-infected cells which may partly explain the functional differences observed in our experiments.

Materials and methods

Design and production of rSFV particles: We used Semliki forest virus (SFV) based replicons that are non-replicating RNA-based virus particles capable of a single round of infection. The viruses were produced as described earlier[25] in BHK21 cells by transfection in the presence of a helper plasmid that encodes structural

proteins for virus assembly and release. The rSFV particles thus produced can encode one transgene for a specific function (*gfp* for this study). Here, GFP (green fluorescent protein) works as a fluorescent marker to measure virus infectivity.

Cell lines and culture: B16F10 cells representing murine metastatic melanoma were cultured in RPMI media with 10% fetal bovine serum depleted of vesicles (see below) and were routinely tested for mycoplasma.
Bone marrow cells isolated from the femur of C57BL6 mice (6-8 weeks old, male) were differentiated into naïve macrophages (M0-like) in the presence of supernatant from L929 cells containing macrophage-colony stimulating factor. Thereafter these macrophages were matured into M2-like macrophages (24 hours treatment with IL4 (50 ng/ml)) or M1-like macrophages (24 hours treatment with interferon-gamma (50 ng/ml) and lipopolysaccharide (2 µg/ml)) for further use. Splenocytes were isolated from C57BL6 mice (6-8 weeks old, male) and immediately used for the experiments. Macrophages and splenocytes were cultured in RPMI media with 10% fetal bovine serum depleted of vesicles. Splenocytes were cultured in the presence of 50 µM of β-mercaptoethanol. Of note, all experiments were carried out using serum depleted of vesicles, except in the case of passaging cells and during freeze-thaw cycles. To exclude EVs present in serum, ultra-centrifugation was carried out at 100,000 g for 16h at 4 °C (Beckman Coulter Optima XE-90, rotor SW28, USA).

Isolation and physical characterization of EVs: 2 million B16F10 cells per flask (175cm^2) were plated and cells were infected after 16 hours of plating with 20 million virus replicon particles (MOI 10) per flask. For EVs isolation, after 24 hours post-infection, cell culture media were consecutively centrifuged at 300 g for 10min, at 2,000 g for 15min, and at 10,000 g for 30min at 4 °C. Then, the supernatant was ultra-centrifuged at 100,000 g for 2 hours (Beckman Coulter Optima XE-90, rotor SW28, USA). The pellet enriched in EVs was washed once with PBS, submitted to ultracentrifugation at the same conditions and subsequently resuspended in PBS and stored at (-20°C). For particle size distribution and concentration quantification, samples were diluted in PBS and loaded into NanoSight NS300 (Malvern, UK) using a syringe pump. Nanoparticle movement was captured for 60 seconds at 25 °C for 5 times. Recorded videos were subjected to Nanoparticle

Tracking Analysis (NTA) Software which determined the size distribution and concentration of EVs.

Western blot of EVs: EVs were sonicated (3 pulses of 5 s at low amplitude) using a probe sonicator (Fisher Brand). Then, samples were loaded onto 10% SDS-PAGE (0.375 M Tris, pH 8.8, 0.1% SDS, 10% acrylamide, 0.03% ammonium persulfate, and 0.06% N, N, N', N'-tetramethyl ethylenediamine). After electrophoresis, the separated proteins were transferred onto PVDF membrane (GE Healthcare) and the membrane was blocked with 5% BSA in 0.1% TBS-Tween for 1h at room temperature. Next, immunoblotting was performed with anti-CD63 (1:700, Thermo Fischer Scientific) and anti-CD9 (1:500, Thermo Fischer Scientific) overnight at 4^{o}C and secondary antibody incubation (1:7000, anti-rabbit IgG Peroxidase, Sigma) for 1h at room temperature. Protein bands were detected with a chemiluminescent kit (Ge Healthcare).

Staining and EVs uptake assay: EVs were stained with PKH26 (Sigma, St. Louis, MO), according to the manufacturer's recommendations. B16F10 cells were incubated overnight with 10^8 EVs/ml concentrations of stained EVs. Images were collected via EVOS microscopy platform (Thermo Fischer Scientific). Uptake of vesicles by individual cells was analyzed using Cell Profiler software (www.cellprofiler.org) by manually labeling individual cells and quantifying the number of (PKH26+) fluorescent spots per cell.

In vivo tumor engraftment: B16F10 cells were treated in vitro with vesicles (10^7 EVs/ml) every day for 5 days and then later collected for subcutaneous tumor engraftment in C57BL6 mice (male, 7 weeks old) in the ventral region of each animal. Mice were s.c. injected with 0.2 million cells resuspended in RPMI media and animals were monitored daily. Tumor growth in time was monitored by performing tumor measurements using a digital caliper. Animals with a measurable tumor (>100 mm^3) were considered to have a successful engraftment, followed by a Kaplan-Meier analysis to determine changes in the probability of tumor engraftment in time due to the pretreatment by EVs from infected cells. Tumor growth rate was assessed by starting the measurement when tumors become measurable (>100 mm^3) and continuing until the tumors reach or exceed a size of 1 cubic centimeter. Animals were kept under a 12:12 light-dark cycle with food and water ad libitum. *In vivo* experiments were

conducted according to legislation for animal research in Brazil with approval from the Committee on Ethics of Animal Experiments of the University of São Paulo (process number 1808/2022).

Clonogenic assay: B16F10 cells were treated with vesicles (10^7 EVs/ml) every day for 5 days and/or treated with rSFV particles (MOI-10) at day 4 in the presence of EVs (supplementary figure 3). After treatment, 200 cells were plated in a 6-well plate and when colonies in the control group reached around 30 to 50 cells (7 days), the cells were washed with PBS and fixed with PBS/formaldehyde 4% for 15 minutes. Cells were washed again with PBS and incubated with crystal violet 0.1% for 10 minutes. After three washes with PBS, the plate was left to dry and then colonies were counted. The assay was performed according to the instructions provided by Franken and colleagues.[26]

Resistance to viral infection assay: 6 x10^3 B16F10 cells were treated daily for 3 days with different concentrations of EVs (10^8-10^9 EVs/ml) from infected or uninfected cells. Then 15 x10^3 of these pre-treated B16F10 cells were re-plated per well in a 96-well plate in the presence of EVs. Upon reaching a confluence of 70%, these cells were infected with rSFV-GFP (MOI-10), again in the presence of fresh EVs (10^8-10^9 EVs/ml). 24 hours after infection, cells were detached and resuspended in PBS for analysis of GFP+ cells by flow cytometry (Attune, Thermo Fischer Scientific).

Macrophage phenotype assay: Bone marrow-derived cells were collected from C57BL/6 mice femur (male, 7-8 weeks old) and cultivated with RPMI media containing 30% L929-conditioned media and 15% FBS for 6 days. Then, one million cells were incubated with Fc block (1 µg) for 1 h at 4°C. Next, anti-F4/80-PE (0.25 µg; BD Biosciences) or isotype control (0.25 µg; anti-rat-IgG2a, ThermoFisher Scientific) was added to samples for 45 min at 4°C and immunostaining of F4/80 positive cells, representing macrophages, were quantified by flow cytometry (Attune, Thermo Fischer Scientific). To address the role of EVs on macrophage polarization, F4/80$^+$ macrophages were plated (4 million cells per plate) in RPMI supplemented with 10% FBS for M0, LPS (1 µg/mL; Sigma) and IFN-γ (50 ng/mL) for M1 or IL-4 (50 ng/mL; R&D Systems) for M2 during 24 hs. Then, M0-like, M1-like or M2-like macrophages were treated with EVs (10^8 EVs/ml) from infected or uninfected cells for 24 hours. After treatment,

cells were detached and processed for RNA extraction using TRIzol according to manufacturer's instructions (Thermo Fischer Scientific). cDNA was synthesized using 2 µg of isolated RNA using High capacity kit (Thermo Fischer Scientific) and Real-Time PCR was performed using SyBR Green chemistry (Thermo Fischer Scientific). Primers used for murine markers are as follows:

- IL-12
  - (Forward: 5'-AGCAGTAGCAGTTCCCCTGA-3'
  - Reverse: 5'-AGTCCCTTTGGTCCAGTGTG-3'),
- iNOS
  - (Forward 5'-CAGGAACCTACCAGCTCACTCT-3'
  - Reverse 5'-ATGTGCTGAAACATTTCCTGTG-3'),
- MRC1
  - (Forward 5'-TTTGCAAGCTTGTAGGAAGGA-3'
  - Reverse 5'-CCAATCCACAGCTCATCATTT-3'),
- Arginase-1
  - (Forward 5'-GAACCCAACTCTTGGGAAGAC-3'
  - Reverse 5'-GGAGAAGGCGTTTGCTTAGTT-3')
- IL-10
  - (Forward 5'-ACTTGCTCTTGCACTACCAAAGCC-3'
  - Reverse 5'-GCATGTGGCTCTGGCCGACTG-3')
- HPRT as endogenous control
  - (Forward 5'-AGGCCAGACTTTGTTGGATTT-3'
  - Reverse 5'-GGCTTTGTATTTGGCTTTTCC-3')

The relative gene expression (fold change) was obtained by the 2^-delta-delta Ct method, according to Livak and Schmittgen and cells treated with EVs from uninfected cells were used as reference sample.[27]

Splenocyte proliferation assay: 10 to 15 million freshly isolated splenocytes were labeled with CFSE (2.5 µM; Thermo Fischer Scientific) for 10 minutes and then stimulated with a combination of phorbol myristate acetate (PMA, 10 µg/ml) and ionomycin (250 ng/ml) in RPMI media with 10% FBS and (50 µM) β-mercaptoethanol. Thereafter, 0.2 million splenocytes per condition per well were allowed to proliferate for 48 hours in the presence of different EVs (10^8/ml). After treatment, cells were resuspended in PBS and processed for flow cytometry

(Attune, Thermo Fischer Scientific) to observe proliferation profile based on CFSE. The protocol was performed as per the instructions provided by Quah and colleagues.[28]

Quantification of microRNAs from in vitro EV-preparations: EVs from infected or non-infected B16F10 cells *in vitro* were processed for microRNA extraction using specific kits (miRNeasy Tissue/Cells Advanced Mini Kit, Qiagen). EVs or tumor tissue microRNA content was performed using MOUSE V1.5 MIRNA ASSAY CSO (Nanostring Technologies) through hybridization with specific probes attached to barcodes on their corresponding microRNA targets. After the detection and acquisition of images for individual counting of molecules, data were analyzed using the nSolver software analysis platform v3.0. The geometric mean from negative control probes was used as a threshold to avoid false positives. Data were then normalized using the most stable microRNAs between groups as an endogenous control to determine the most abundant miRs in each group.

Statistical analysis: One-way ANOVA was used to calculate significance. Statistical differences were considered when $p \leq 0.05$ and Bonferroni's correction was applied for multiple comparisons.

Results

Isolation and physical characterization of EVs released upon SFV-infection

Replicating wild-type SFV infection has been associated with changes in the expression of genes involved in the regulation of EV synthesis and release (Supplementary Figure 1), indicating that EVs from healthy albeit infected cells may have a different composition or function as compared to non-infected cells. Therefore, we first set out to isolate and characterize EVs released from melanoma cells post viral infection. We infected B16F10 melanoma cells with an MOI-10 of rSFV encoding GFP (SFV-GFP) (Figure 1A) and performed a PBS-wash after 2 hours of infection to remove extracellular rSFV particles from the supernatant. 24 hours post-infection, the supernatant was collected and the EVs were isolated through serial ultracentrifugation (Figure 1B). Between independent batches of EV preparations, we observed minimal variations in the overall yield of EVs obtained

from infected (SFV EVs) and non-infected cells (NT EVs) (Figure 1C). However, considering the reduction in cell numbers due to oncolysis in the rSFV-infected condition, we noticed a substantial increase in the vesicle-per-cell ratio from infected cells compared to non-infected cells (Figure 1D-E).

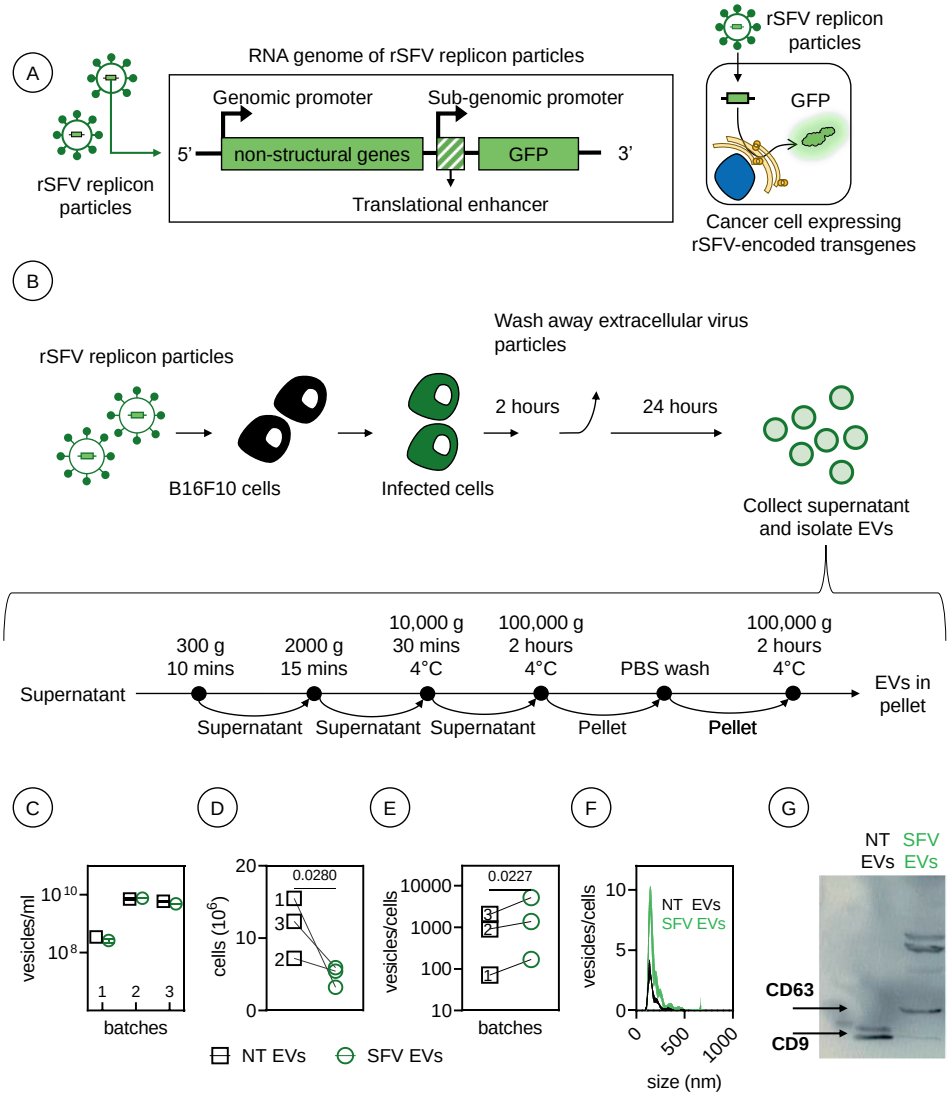

Figure 1: Isolation and characterization of tumor-derived EVs upon exposure to rSFV replicon particles. (A) Semliki Forest virus replicon particles were engineered by replacing the structural genes in the genome with a GFP-transgene (left) to enable a single round of infection (right). (B) Illustration of the experimental scheme for rSFV infection of B16F10

cells followed by a wash 2 hours post-infection to remove extracellular virus particles and incubation for 24 hours before the collection of supernatants followed by EV isolation through sequential ultracentrifugation steps. (C) Absolute vesicle yield from infected (rSFV EVs) or non-infected B16F10 cells (NT EVs) in different batches. (D) Decrease in the number of viable B16F10 cells upon rSFV infection. (E) Vesicles per cell count based on number of cells present at the time of EV isolation. (F) Size distribution of EVs from infected and non-infected cells. (G) Western blot image for validation of expression of CD63 and CD9 as EV membrane markers in the EV-preparations. In (C-E) n=3 independent batches of EV-preparation are shown. Data are presented as mean values.

B16F10 cells produced a heterogeneous population of EVs with most of the EVs being around 200 nm in diameter, with infected cells notably producing larger-sized EVs as well (>300 nm diameter) (Figure 1F). Through western blot, we validated the presence of tetraspanins (vesicle membrane-associated proteins) in EV preparations; where EVs from infected cells were enriched in CD63 membrane proteins as compared to CD9 enriched EVs from non-infected cells (Figure 1G). The presence of multiple CD63 bands is often associated with the existence of isoforms, which can be attributed to variations in its glycosylation status. (doi: 10.1186/1476-4598-13-134) The CD63 enrichment in SFV EVs paralleled the CD63 upregulation observed in SFV-infected cells (Supplementary Figure 1).

Effect of SFV EVs on melanoma cells

Melanoma EVs have the potential to transfer pro-tumoral survival signals to recipient melanoma cells and promote tumor progression.[29–31] Therefore, we tested if rSFV-infection could alter the communication dynamics or the pro-tumoral potential of melanoma EVs. First, we labeled SFV- or NT EVs with a lipophilic dye and quantified their uptake by B16F10 melanoma cells (Supplementary Figure 2A-B), where we observed that B16F10 melanoma cells did not exhibit significant differences in the uptake of EVs produced by infected or non-infected cells (Supplementary Figure 2C). Moreover, EVs from infected cells did not show cytotoxic effects on the B16F10 cells (Supplementary Figure 2D). We next evaluated if EVs from infected cells influenced the process of tumor development through an *in vivo* experiment. We treated B16F10 cells every 24 hours with EVs for 5 days and then grafted them subcutaneously in C57BL6 mice

to study the efficacy of tumor engraftment (Figure 2A). B16F10 melanoma cells treated with EVs from non-infected cells developed tumors in all mice, in contrast to treatment with EVs from SFV-infected cells, where 40% of the animals did not develop tumors upto 40 days after injection (Figure 2B), indicating that EVs from infected cells might impair melanoma engraftment. Although we observed a delay in engraftment, the rate of tumor growth was not significantly different when measured from the point at which tumors became measurable and tracked until they reached or surpassed a size of 1 cubic centimeter. (Figure 2C).

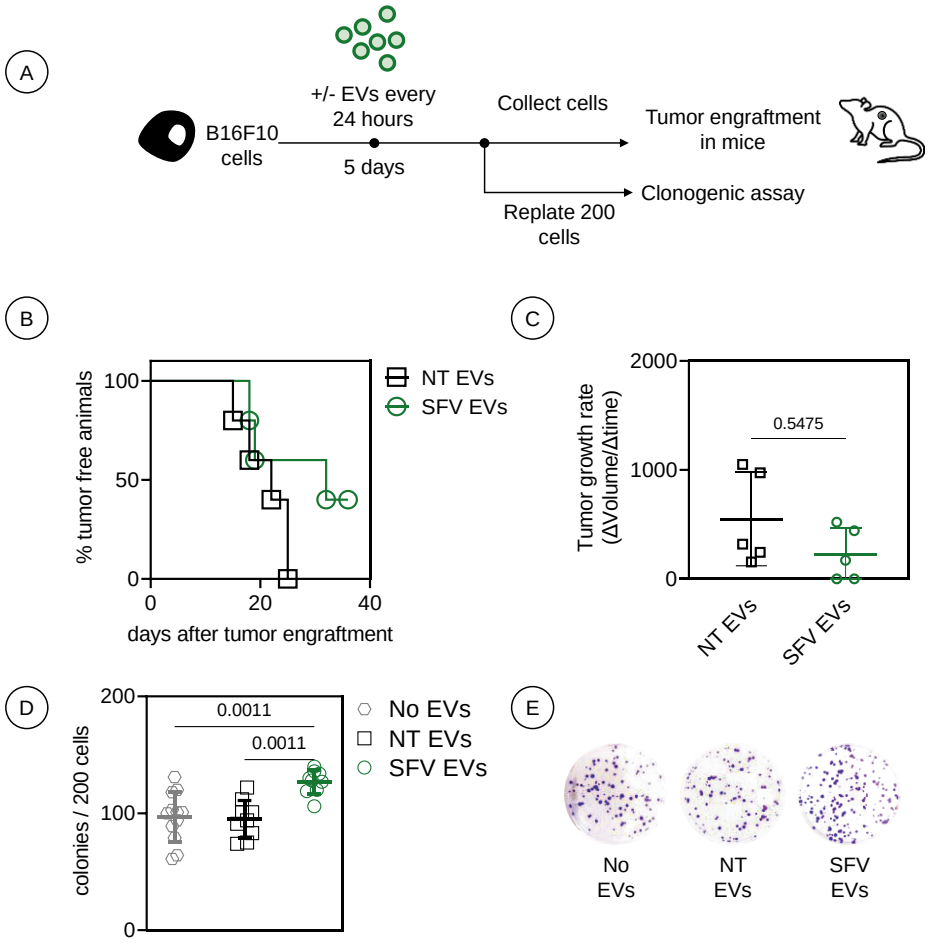

Figure 2: The effect of rSFV-induced EVs on tumor establishment. (A) Overall scheme of the experimental steps where B16F10 cells were pre-treated with EVs from infected (SFV EVs) or non-infected cells (NT EVs) daily for 5 days and then collected for an in vivo tumor engraftment assay or an in vitro clonogenic assay. (B) Percentage of animals free from tumor and (C) related tumor growth rate upon injection with B16F10 cells pretreated with

SFV EVs or NT EVs (n=5 for each group). (D) Frequency of colonies formed from 200 cells plated after 7 days of clonogenic assay. (E) Representative images of colonies in a well formed by B16F10 cells from different conditions. In (D-E) n=12 replicates from 4 independent experiments. One-way ANOVA followed by Bonferroni's multiple comparisons test was performed. Data are presented as mean values ± SD.

To investigate if EVs from infected cells negatively influenced the tumorigenic potential of melanoma cells, we performed an *in vitro* experiment to assess their clonogenic potential. Interestingly, in contrast to the results from the *in vivo* experiment, EVs from infected cells led to a significant increase of 25% in the number of B16F10 colonies as compared to EVs from non-infected cells (Figure 2D-E). Simultaneously, we tested if EVs from infected cells could confer resistance to infection in recipient melanoma cells and thereby improve tumor survival (Supplementary Figure 3A). Pre-treatment of B16F10 melanoma cells with EVs from infected cells did not lead to resistance but rather led to a 5-10% increase in the susceptibility to virus infection as quantified through the number of GFP-positive cells (Supplementary Figure 3B-C). Of note, GFP expression was not observed in melanoma cells upon treatment with EVs alone. Moreover, pre-treatment with EVs from infected cells also did not alter the susceptibility of cells to rSFV-mediated impairment of tumor clonogenicity (Supplementary Figure 3D-E).

Effect of SFV EVs on modulating macrophage polarization

Considering the impairment in tumor engraftment by EVs from infected cells, we hypothesized that this may result from a systemic modulation of the tumor microenvironment and immune cells instead of through alterations in the clonogenic potential of melanoma or their sensitivity to virus infection. Tumor EVs have been described to regulate the activity of tumor-associated myeloid cells and to alter their phenotype to a more M2-like wound-healing and regulatory profile, rather than an M1-like inflammatory profile.[32–34] Therefore, we tested if rSFV infection could alter melanoma EVs and regulate the macrophage phenotype to a pro-inflammatory type. For this, bone-marrow-derived murine macrophages were polarized to either an M1-like or M2-like phenotype through cytokine stimulation in the presence of EVs from infected or non-infected cells (Figure 3A). In

macrophages initially polarized towards an M2-like phenotype, we observed that EVs from melanoma cells further promoted the regulatory phenotype through upregulation of MRC-1 (CD206) and arginase (Arg-1) gene expression and an observable but statistically insignificant downregulation of IL-12 and iNOS expression (Figure 3B-E). In contrast, EVs from infected cells demonstrated more pro-inflammatory effects by inhibiting the upregulation of MRC-1 and arginase expression and a trend towards promoting IL-12 and iNOS expression. Alternatively, in naive M0-like or M1-like macrophages EVs from melanoma cells upregulated the expression of iNOS, indicating a context-dependent or mixed functional profile (Figure 3E).

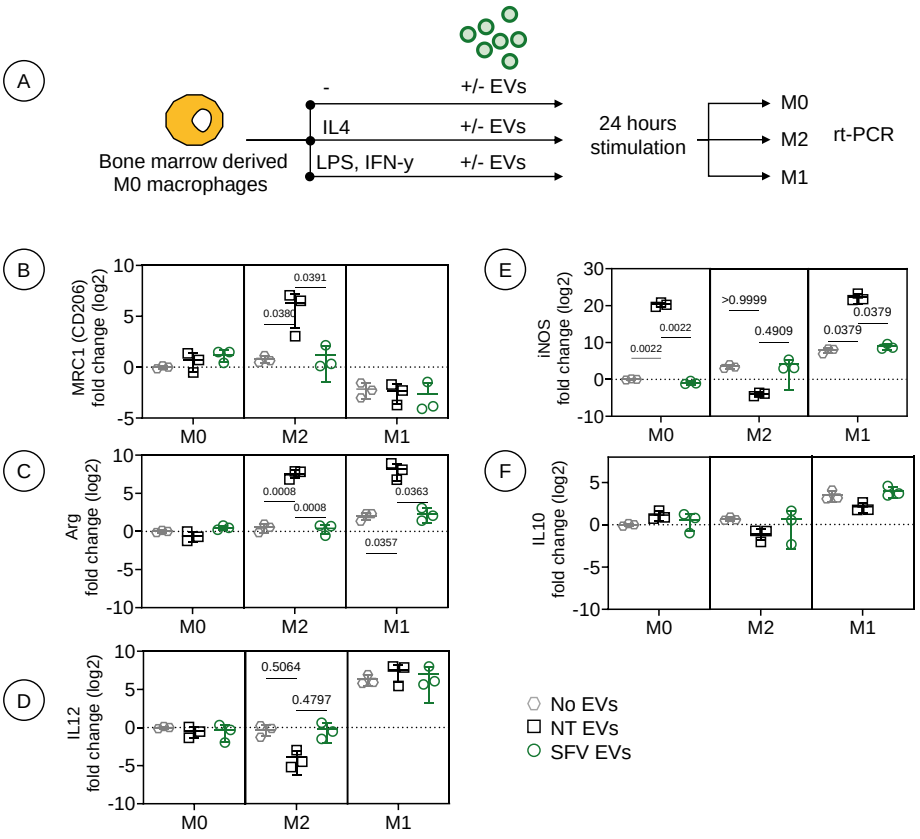

Figure 3: The effect of rSFV-induced EVs on macrophage polarization. (A) Illustration of the experiment where bone-marrow derived macrophages were polarized to inflammatory M1-like or regulatory M2-like macrophages in presence of EVs from infected (SFV EVs) or non-infected cells (NT EVs). Polarization towards an M1-like phenotype was done through treatment with LPS and IFN-y, while towards an M2-like phenotype was done with IL-4.

Macrophage polarization was assessed by quantification of mRNA expression of (B) mrc1, (C) arg1, (D) il12, (E) inos, and (F) il10, with hprt used as an endogenous housekeeping gene. In (B-F) bone-marrow derived macrophages tested from n=3 animals in independent experiments. Data are presented as mean values ± SD.

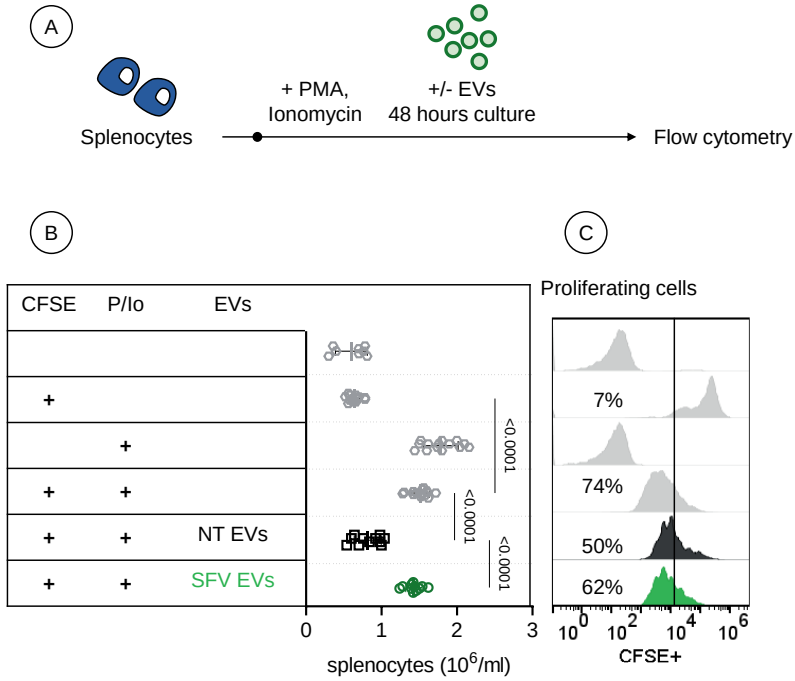

Figure 4: The effect of rSFV-induced EVs on splenocyte activation and proliferation. (A) Illustration of the experimental steps where freshly isolated splenocytes from mice were labeled with CFSE and then activated with PMA and ionomycin in the presence of EVs from infected (SFV EVs) or non-infected cells (NT EVs). 48 hours post treatment, CFSE-labeled splenocytes were (B) counted manually and (C) analyzed by flow cytometry to observe CFSE-based proliferation profiles. Splenocytes were isolated from n=4 animals for independent experiments. Data are presented as mean values ± SD.

Effect of SFV EVs on the activation of splenocytes

In addition to myeloid cells, melanoma EVs have also been reported to regulate activation and regulation of lymphocyte function in tumors.[24,35] So, we hypothesized that changes in melanoma EVs induced by rSFV infection may also influence the regulation of lymphocyte activation. We studied lymphocyte activation through mitogenic stimulation of splenocytes and measured splenocyte proliferation in the presence of melanoma EVs (Figure 4A). We observed that

melanoma EVs significantly reduced the activation-induced proliferation of splenocytes, whereas the magnitude of inhibition was not as strong in the case with EVs from infected cells (Figure 4B-C). Through absolute count of splenocytes and CFSE-based analysis of cell proliferation, we confirmed that melanoma EVs slowed down the proliferative potential of splenocytes.

Differences in the microRNA cargo of SFV EVs

The current literature in the field of EVs has shown that EVs confer changes in functional phenotypes of recipient cells through various biochemical signals in the form of lipids, proteins, and nucleotides, among others.[20] Recently, there has been an increased interest in studying the role of non-coding RNA sequences, e.g. microRNAs that are transferred through EVs, which can potentially regulate gene expression in target cells. Moreover, some studies have shown that microRNA transfer from infected cells to other cancer cells can further sensitize the cells for infection and that one can engineer viruses to exploit the EV-mediated delivery of potential microRNA candidates.[10,12]

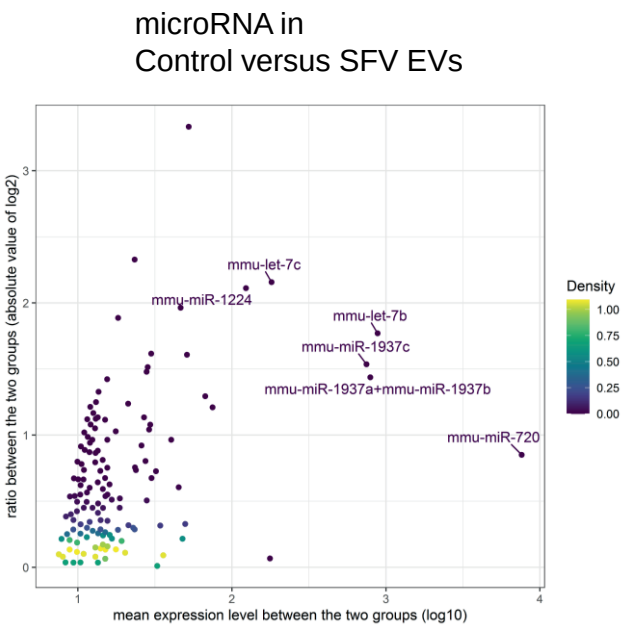

Figure 5: The effect of viral infection in reprogramming the microRNA cargo of EVs. Density map showing miRNAs profile comparing microRNA ratio between control EVs versus SFV EVs.

In order to find anti-tumoral and pro-immunogenic microRNA candidates present in the EVs, we characterized the microRNA cargo of EVs derived from infected cells. We observed that rSFV infection indeed caused differences in microRNAs packaged in the EVs as compared to the ones from uninfected cells (Figure 5A). Specifically, we found that microRNAs from the let-7 family were significantly enriched in EVs from uninfected cells suggesting that the presence of rSFV in melanoma cells modify microRNA cargo sorting into EVs through a still unknown mechanism.

Discussion

Our study investigated the effect of rSFV on the characteristics and functionality of EVs released by rSFV-infected melanoma cells. Our results demonstrate that infection with rSFV brought about changes in the physicochemical properties of EVs. This included an increase in their concentration and size, along with alterations in their microRNA cargo. Notably, the sorting of microRNAs in EVs from rSFV-infected cells was found to be different, indicating that virotherapy can influence the packaging of specific microRNAs within EVs. Moreover, we observed that these EVs from rSFV-infected melanoma cells reduced tumor engraftment in mice. This effect could be partially attributed to the pro-inflammatory properties of the EVs, where they supported the activation of splenocytes and promoted the polarization of macrophages towards an inflammatory phenotype. Overall, our findings shed light on how virotherapy based on rSFV affects the cargo and function of EVs, highlighting their potential role in modulating the immune response and tumor progression.

Based on our findings, EVs from rSFV-infected cells have distinct features compared to EVs from uninfected cells. Specifically, EVs from infected cells were enriched in exosomal markers (CD63), while those from uninfected cells were enriched in ectosomal markers (CD9).[36] Our data also suggest a slight increase (5%) in infectivity by SFV-GFP particles upon preincubation of melanoma cells with EVs from infected cells. This might be partly explained by the fact that CD63 has been found to be involved in several stages of exosomal release and its enrichment in EVs positively correlates with virus infection and spread.[37–40]

Moreover, our study found that rSFV infection of melanoma cells impacted the packaging of specific microRNAs in EVs. This is consistent with previous studies that have reported the selective sorting of miRs into EVs upon viral infection.[10] Interestingly, some miRs were found to be less abundant in the EVs from infected cells. This might suggest miR-dependent phenotypic differences in the recipient cells that we observed in our study, where miRs could potentially regulate the survival of cancer cells or the activation profile of immune cells.[41,42] MicroRNA-mediated sensitization of cancer cells towards viral infection may be another explanation for improved infectivity by rSFV in melanoma cells. Future studies could investigate in more depth the specific factors transferred by EVs and their contribution to therapy resistance.

We observe that virus infection does not only alter the cargo of EVs but also impacts the phenotype of recipient cells. For example, EVs from rSFV-infected cells slightly enhanced the clonogenic potential of recipient melanoma cells. We can assume that this minor increase might possibly result from a few melanoma clones that benefitted in survival through reprogramming mediated by EVs. Although an increased survival may hint towards the development of resistance to virotherapy, we found that the sensitivity of melanoma cells towards rSFV infection remained unaltered. This could be explained by the fact that EVs from melanoma cells, which are known to transfer pro-survival signals,[20,21] may be enriched with such signals upon virus infection.

In addition, our results show that rSFV infection influenced an immunomodulatory profile of melanoma EVs. Previously, EVs from B16F10 cells have been reported to have an immunosuppressive role by inducing T cell exhaustion and reprogramming macrophages to a regulatory state.[22,33,35] In line with these findings, we also observed melanoma EVs to bear an immunosuppressive profile, however, this was not the case for rSFV-induced EVs. It could be hypothesized that this effect is partly due to altered biogenesis and/or EV cargo in rSFV-infected cells. For example, human melanoma EVs have been reported to carry regulatory checkpoint markers like PDL-1 and CD206 which may not be enriched in EVs from infected cells.[22] Whereas upon infection, cancer cells may secrete EVs with a virus-related cargo, such as single- or double-stranded RNAs and viral proteins, which in turn can activate innate pathogen recognition receptors in immune cells.[3,43]

Investigating the specific factors transferred by EVs that contribute to the immunogenic effects observed in SFV EVs would be the focus of future research as it may aid in the development of novel therapeutic strategies.

Although our study focused on the effects of virotherapy using rSFV on melanoma EVs, our findings can contribute to a broader understanding of how viral infection impacts EV composition and function in cancer. And importantly to note that the use of rSFV ensures that infected cells do not produce virus, which in this study and experimental set up allowed for the isolation and systematic characterization of vesicles without virus contamination. Our results provided important insights into the immediate effects of rSFV-mediated virotherapy on the functional profile of EVs, including their microRNA cargo. In conclusion, our study provides evidence that oncolytic virotherapy can alter the biogenesis and cargo of EVs released by cancer cells. Our findings suggest that rSFV-induced immunogenic alterations in EVs could potentially influence the tumor microenvironment and could impact the response to therapy. Therefore, we support further investigation into the role of EVs in virotherapy to fully understand the impact of these vesicles on tumor progression and therapeutic outcomes.

Acknowledgements

We acknowledge all members of the technical support from our institute, CTO-ICESP, Prof. Dr. Ana Paula Lepique (ICB-IV, USP) for the guidance in the flow cytometry analysis, and the technical assistance provided by Márcio de Carvalho from Nanostring Core (Experimental Research Unity, UNESP).

Declaration of interest

The authors report there are no competing interests to declare.

Funding

This research was supported by grants from FAPESP (Fundação de Amparo a Pesquisa do Estado de São Paulo, grant Number 2020/09176-8), CAPES (Coordenação de Aperfeiçoamento de Pessoal de Nível Superior) PhD scholarship for DB, and GSMS-ATTP (University of Groningen, Graduate school of Medical Sciences, Abel Tasman Talent program) PhD scholarship for DB.

References

1. Cocozza, F., Grisard, E., Martin-Jaular, L., Mathieu, M. & Théry, C. SnapShot: Extracellular Vesicles. *Cell* **182**, 262-262.e1 (2020).
2. Colombo, M., Raposo, G. & Théry, C. Biogenesis, Secretion, and Intercellular Interactions of Exosomes and Other Extracellular Vesicles. *Annual Review of Cell and Developmental Biology* **30**, 255–289 (2014).
3. Pegtel, D. M. & Gould, S. J. Exosomes. *Annu Rev Biochem* **88**, 487–514 (2019).
4. Schorey, J. S., Cheng, Y., Singh, P. P. & Smith, V. L. Exosomes and other extracellular vesicles in host-pathogen interactions. *EMBO Rep* **16**, 24–43 (2015).
5. Alenquer, M. & Amorim, M. Exosome Biogenesis, Regulation, and Function in Viral Infection. *Viruses* **7**, 5066–5083 (2015).
6. Dogrammatzis, C., Waisner, H. & Kalamvoki, M. Cloaked Viruses and Viral Factors in Cutting Edge Exosome-Based Therapies. *Front Cell Dev Biol* **8**, 376 (2020).
7. Lv, P. *et al.* Genetically Engineered Cell Membrane Nanovesicles for Oncolytic Adenovirus Delivery: A Versatile Platform for Cancer Virotherapy. *Nano Lett* **19**, 2993–3001 (2019).
8. Ruiz-Guillen, M. *et al.* Capsid-deficient alphaviruses generate propagative infectious microvesicles at the plasma membrane. *Cell Mol Life Sci* **73**, 3897–3916 (2016).
9. Saari, H. *et al.* Extracellular vesicles provide a capsid-free vector for oncolytic adenoviral DNA delivery. *J Extracell Vesicles* **9**, 1747206 (2020).
10. Zhou, C. *et al.* Exosomes Carry microRNAs into Neighboring Cells to Promote Diffusive Infection of Newcastle Disease Virus. *Viruses* **11**, E527 (2019).
11. Labani-Motlagh, A., Naseri, S., Wenthe, J., Eriksson, E. & Loskog, A. Systemic immunity upon local oncolytic virotherapy armed with immunostimulatory genes may be supported by tumor-derived exosomes. *Mol Ther Oncolytics* **20**, 508–518 (2021).
12. Wedge, M.-E. *et al.* Virally programmed extracellular vesicles sensitize cancer cells to oncolytic virus and small molecule therapy. *Nat Commun* **13**, 1898 (2022).
13. Nolte-'t Hoen, E., Cremer, T., Gallo, R. C. & Margolis, L. B. Extracellular vesicles and viruses: Are they close relatives? *Proc. Natl. Acad. Sci. U.S.A.* **113**, 9155–9161 (2016).
14. Zhou, Y., McNamara, R. P. & Dittmer, D. P. Purification Methods and the Presence of RNA in Virus Particles and Extracellular Vesicles. *Viruses* **12**, 917 (2020).
15. Kakiuchi, Y. *et al.* Local oncolytic adenovirotherapy produces an abscopal effect via tumor-derived extracellular vesicles. *Mol Ther* **29**, 2920–2930 (2021).
16. Smerdou, C. & Liljeström, P. Two-helper RNA system for production of recombinant Semliki forest virus particles. *J Virol* **73**, 1092–1098 (1999).
17. Liljeström, P. & Garoff, H. A new generation of animal cell expression vectors based on the Semliki Forest virus replicon. *Biotechnology (N.Y.)* **9**, 1356–1361 (1991).
18. Singh, A., Koutsoumpli, G., van de Wall, S. & Daemen, T. An alphavirus-based therapeutic cancer vaccine: from design to clinical trial. *Cancer Immunol Immunother* **68**, 849–859 (2019).
19. Zhou, Q. *et al.* Tumor-derived extracellular vesicles in melanoma immune response and immunotherapy. *Biomed Pharmacother* **156**, 113790 (2022).
20. Santos, N. L., Bustos, S. O., Bhatt, D., Chammas, R. & Andrade, L. N. de S. Tumor-Derived Extracellular Vesicles: Modulation of Cellular Functional Dynamics in Tumor Microenvironment and Its Clinical Implications. *Front. Cell Dev. Biol.* **9**, 737449 (2021).
21. Andrade, L. N. de S. *et al.* Extracellular Vesicles Shedding Promotes Melanoma Growth in Response to Chemotherapy. *Sci Rep* **9**, 14482 (2019).
22. Chen, G. *et al.* Exosomal PD-L1 contributes to immunosuppression and is associated with anti-PD-1 response. *Nature* **560**, 382–386 (2018).
23. Poggio, M. *et al.* Suppression of Exosomal PD-L1 Induces Systemic Anti-tumor Immunity and Memory. *Cell* **177**, 414-427.e13 (2019).
24. Chen, J. *et al.* Tumor extracellular vesicles mediate anti-PD-L1 therapy resistance by decoying anti-PD-L1. *Cell Mol Immunol* **19**, 1290–1301 (2022).

25. Daemen, T., Regts, J., Holtrop, M. & Wilschut, J. Immunization strategy against cervical cancer involving an alphavirus vector expressing high levels of a stable fusion protein of human papillomavirus 16 E6 and E7. *Gene Ther* **9**, 85–94 (2002).
26. Franken, N. A. P., Rodermond, H. M., Stap, J., Haveman, J. & van Bree, C. Clonogenic assay of cells in vitro. *Nat Protoc* **1**, 2315–2319 (2006).
27. Livak, K. J. & Schmittgen, T. D. Analysis of relative gene expression data using real-time quantitative PCR and the 2(-Delta Delta C(T)) Method. *Methods* **25**, 402–408 (2001).
28. Quah, B. J. C., Warren, H. S. & Parish, C. R. Monitoring lymphocyte proliferation in vitro and in vivo with the intracellular fluorescent dye carboxyfluorescein diacetate succinimidyl ester. *Nat Protoc* **2**, 2049–2056 (2007).
29. Cheng, Y.-C. *et al.* The Roles of Extracellular Vesicles in Malignant Melanoma. *Cells* **10**, 2740 (2021).
30. Hood, J. L. Natural melanoma-derived extracellular vesicles. *Semin Cancer Biol* **59**, 251–265 (2019).
31. Matsumoto, A. *et al.* Accelerated growth of B16BL6 tumor in mice through efficient uptake of their own exosomes by B16BL6 cells. *Cancer Science* **108**, 1803–1810 (2017).
32. Yin, Y. *et al.* Colorectal Cancer-Derived Small Extracellular Vesicles Promote Tumor Immune Evasion by Upregulating PD-L1 Expression in Tumor-Associated Macrophages. *Adv Sci (Weinh)* **9**, 2102620 (2022).
33. Bardi, G. T., Smith, M. A. & Hood, J. L. Melanoma exosomes promote mixed M1 and M2 macrophage polarization. *Cytokine* **105**, 63–72 (2018).
34. Morrissey, S. M. *et al.* Tumor-derived exosomes drive immunosuppressive macrophages in a pre-metastatic niche through glycolytic dominant metabolic reprogramming. *Cell Metab* **33**, 2040-2058.e10 (2021).
35. Gupta, P. *et al.* Tumor Derived Extracellular Vesicles Drive T Cell Exhaustion in Tumor Microenvironment through Sphingosine Mediated Signaling and Impacting Immunotherapy Outcomes in Ovarian Cancer. *Adv Sci (Weinh)* **9**, e2104452 (2022).
36. Mathieu, M. *et al.* Specificities of exosome versus small ectosome secretion revealed by live intracellular tracking of CD63 and CD9. *Nat Commun* **12**, 4389 (2021).
37. Earnest, J. T. *et al.* The tetraspanin CD9 facilitates MERS-coronavirus entry by scaffolding host cell receptors and proteases. *PLoS Pathog* **13**, e1006546 (2017).
38. York, S. B. *et al.* Zika Virus Hijacks Extracellular Vesicle Tetraspanin Pathways for Cell-to-Cell Transmission. *mSphere* **6**, e0019221 (2021).
39. Ninomiya, M. *et al.* The Exosome-Associated Tetraspanin CD63 Contributes to the Efficient Assembly and Infectivity of the Hepatitis B Virus. *Hepatol Commun* **5**, 1238–1251 (2021).
40. Stiles, K. M. & Kielian, M. Role of TSPAN9 in Alphavirus Entry and Early Endosomes. *J Virol* **90**, 4289–4297 (2016).
41. Sun, Z. *et al.* Effect of exosomal miRNA on cancer biology and clinical applications. *Mol Cancer* **17**, 147 (2018).
42. Robbins, P. D. & Morelli, A. E. Regulation of immune responses by extracellular vesicles. *Nat Rev Immunol* **14**, 195–208 (2014).
43. Kouwaki, T., Okamoto, M., Tsukamoto, H., Fukushima, Y. & Oshiumi, H. Extracellular Vesicles Deliver Host and Virus RNA and Regulate Innate Immune Response. *Int J Mol Sci* **18**, 666 (2017).

Supplementary figures

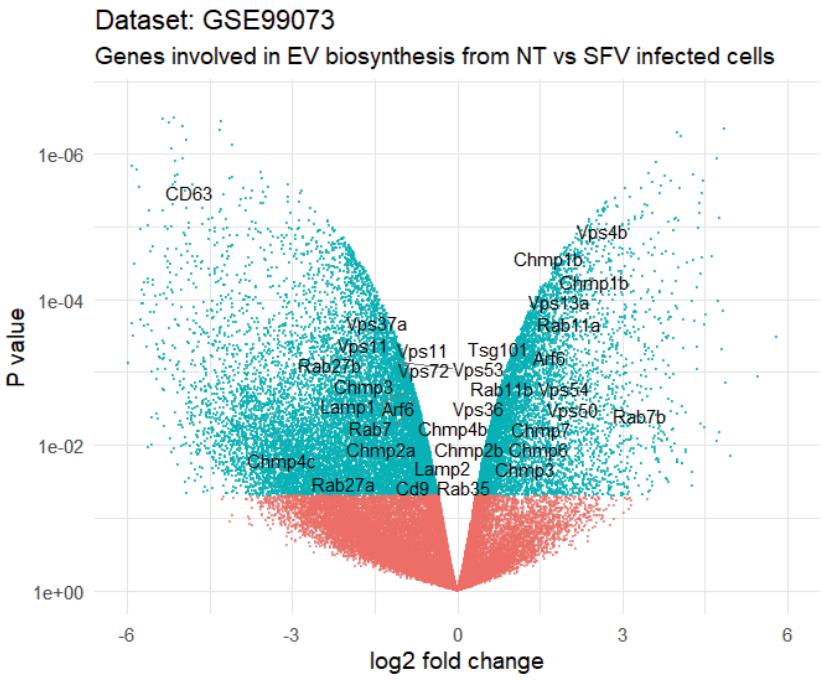

Supplementary Figure 1: Differential expression of genes involved in EV biosynthesis upon wild-type SFV infection. The GSE99073 dataset was analyzed using the GEO2R platform and is represented as a volcano plot of the expression of genes in non-infected (right part) vs SFV-infected cells (left part). The dataset was obtained from a microarray analysis of NIH/3T3 cells infected or not with wild-type SFV. Various genes involved in EV biosynthesis are differentially regulated, including a relatively strong upregulation of CD63 expression upon SFV infection.

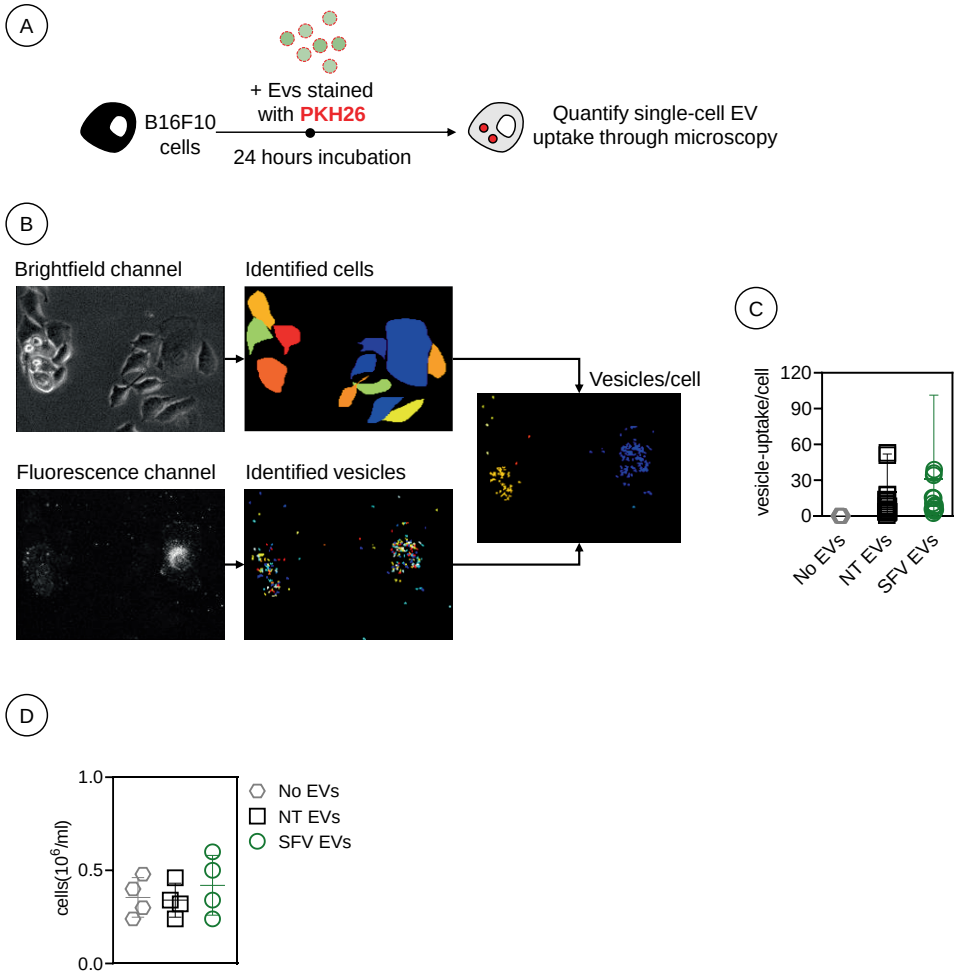

Supplementary Figure 2: Quantifying uptake of EVs by B16F10 cells. (A) Illustration of the experimental steps where EVs from infected (SFV EVs) or non-infected cells (NT EVs) were labeled with PKH26 dye and incubated with B16F10 cells to visualize uptake using microscopy. (B) 24 hours post-incubation, cells were manually identified through brightfield images and PKH26+ spots were quantified using the CellProfiler platform. (C) Frequency of PKH26+ spots per cell represented as vesicle uptake by B16F10 cells. (D) Viability of B16F10 cells after treatment with EVs from infected or non-infected cells. In (D) n=4 independent experiments. Data are presented as mean values ± SD.

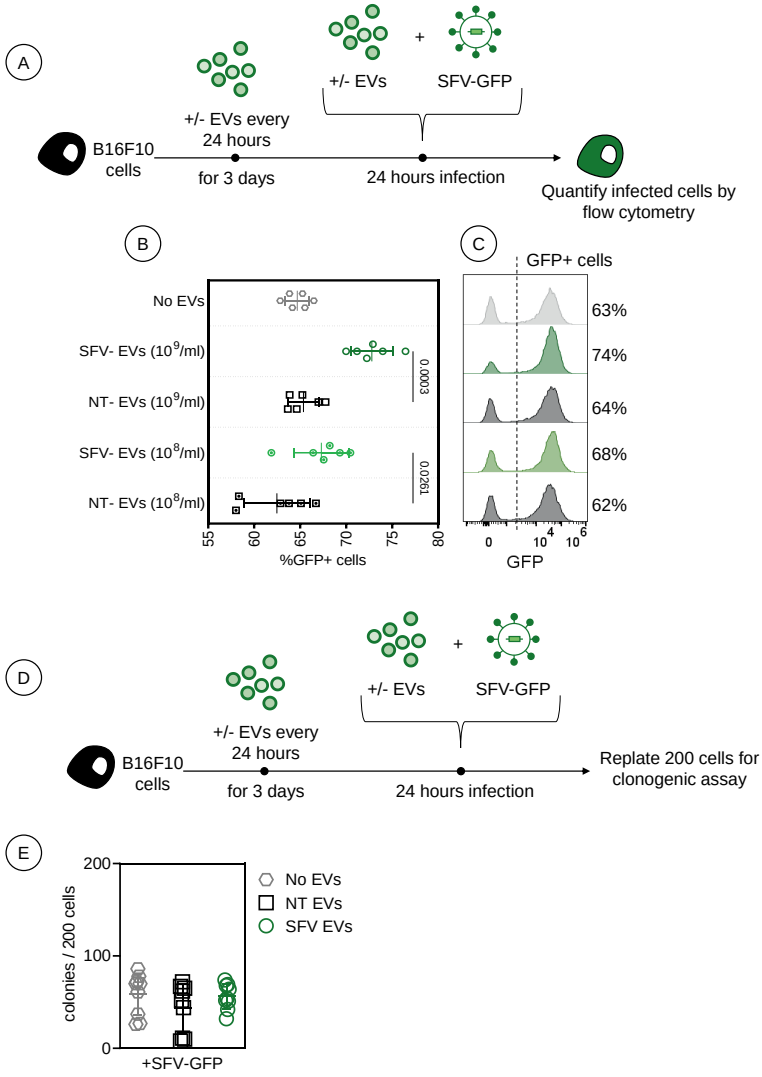

Supplementary figure 3: The effect of rSFV-induced EVs on sensitization of tumor cells to viral infection and tumor clonogenicity. (A) Illustration of the experimental steps where B16F10 cells were pre-treated with EVs from infected (SFV EVs) or non-infected cells (NT EVs), followed by infection with SFV-GFP virus and quantification of cells expressing GFP 24 hours after infection. (B) Percentage of cells expressing GFP after 24 hours of infection. (C) Histogram of GFP expression in cells upon SFV-GFP infection in different conditions. (D) Overall scheme of the experimental steps where B16F10 cells are pre-treated with EVs from infected (SFV EVs) or non-infected cells (NT EVs) daily for 3 days and then infected with rSFV-GFP in the presence of EVs. 24 hours after infection the cells were collected for an in vitro clonogenic assay. (E) Frequency of colonies formed from 200 cells plated after 7 days of clonogenic assay. In (B) n=6 replicates from 3 independent experiments. In (E) n=12 replicates from 4 independent experiments. One-way ANOVA followed by Bonferroni's multiple comparisons test was performed. Data are presented as mean values ± SD.